Locked entropy in partially coherent optical fields

Mitchell Harling, Varun A. Kelkar, Kimani C. Toussaint, Jr., and Ayman F. Abouraddy

Phys. Rev. A **109**, L021501 — Published 8 February 2024

DOI: 10.1103/PhysRevA.109.L021501

Locked entropy in partially coherent optical fields

Mitchell Harling,[1] Varun A. Kelkar,[2,3] Kimani C. Toussaint, Jr.,[1] and Ayman F. Abouraddy[4]

[1] *PROBE Lab, School of Engineering, Brown University, Providence, RI 02912, USA*
[2] *Department of Electrical and Computer Eng., University of Illinois at Urbana-Champaign, Urbana, IL 61801, USA*
[3] *Currently at Algorithmic Systems Group, Analog Garage, Analog Devices, Inc., Boston, MA 02110, USA*
[4] *CREOL, The College of Optics & Photonics, University of Central Florida, Orlando, FL 32816, USA*

(Dated: January 22, 2024)

We introduce a taxonomy for partially coherent optical fields spanning multiple degrees of freedom (DoFs) based on the rank of the associated coherence matrix (the number of non-zero eigenvalues). When DoFs comprise two spatial modes and polarization, a fourfold classification emerges, with rank-1 fields corresponding to fully coherent fields. We demonstrate theoretically and confirm experimentally that these classes have heretofore unrecognized different properties. Specifically, whereas rank-2 fields can always be rendered separable with respect to its DoFs via a unitary transformation, rank-3 fields are always non-separable. Consequently, the entropy for a rank-2 field can always be concentrated into a single DoF (thus ridding the other DoF of statistical fluctuations), whereas some entropy is always 'locked' in one DoF of a rank-3 field. These results offer new insight into the dynamics of optical coherence upon traversing systems or media that couple DoFs.

The study of optical coherence and the statistical fluctuations in optical fields extends back to the pioneering work of Zernike [1], and subsequently reached maturation in the work of Wolf and Mandel [2–4]. Recently, new insights into optical coherence have been brought to light [5, 6] by exploiting the mathematical correspondence between the coherence matrix for classical optical fields involving multiple degrees of freedom (DoFs) [7–9] and the density operator representing multipartite quantum mechanical states. This correspondence has led to the coinage of the term 'classical entanglement' [6, 10–14] to describe optical fields that are *not* separable with respect to their DoFs, in analogy with quantum entanglement that is intrinsic to non-separable multipartite quantum states. The concept of classical entanglement has helped solve problems with regards to Mueller matrices [15], determine the maximum achievable Young double-slit interference visibility [16], and enable the characterization of quantum optical communications channels [17], among many other applications [18–26].

The study of classical entanglement in optical fields is enriched by the possibility of implementing inter-DoF (or global) unitary transformations ('unitaries' henceforth for brevity [16, 27]), including entangling and disentangling unitaries; e.g., a spatial light modulator can entangle or disentangle polarization and spatial modes [28]. This feature is central to the recent demonstration of entropy swapping [29–31], which refers to the reversible reallocation of statistical fluctuations from one DoF to another in a partially coherent field. For example, starting with a *polarized* but spatially *incoherent* field (the entropy is confined to the spatial DoF), a global unitary can convert the field to one that is *unpolarized* but spatially *coherent* (the entropy has been swapped to the polarization DoF with no loss of energy). A similar approach enables entropy concentration, whereby the entropy shared among the DoFs can be optimally transferred into a single DoF via a unitary [30].

Here we uncover a surprising feature of partially coherent optical fields that places a constraint on entropy concentration under arbitrary global unitaries [16, 29]. For concreteness, we examine a canonical optical field model having two binary DoFs, and introduce a fourfold taxonomy based on the *coherence rank* of the associated 4×4 coherence matrix, which corresponds to the number of its non-zero eigenvalues (from 1 to 4). While the rank-1 class embraces all coherent fields, rank-2 through rank-4 classes comprise partially coherent fields. We find that fields of different ranks have altogether different characteristics that have not been investigated to date. Specifically, we find that the potential for concentrating the field entropy into a single DoF depends crucially on the rank. Most conspicuously, the entropy of rank-2 fields – no matter how *high* – can *always* be concentrated into a single DoF, thereby leaving the other DoF free of statistical fluctuations [Fig. 1]. Indeed, there always exists a global unitary that renders the field separable with respect to its DoFs, with all the initial entropy concentrated into a single DoF. In stark contrast, it is *impossible* to concentrate all the entropy of rank-3 fields – no matter how *low* – into one DoF, and residual fluctuations must be retained by the other DoF, which we call 'locked entropy' [Fig. 1]. This stems from the fact that rank-3 fields possess a *fundamentally non-separable* structure that cannot be eliminated unitarily. We demonstrate these effects experimentally using optical fields defined by polarization and two spatial modes as the binary DoFs of interest. These results open a new window onto understanding the dynamics of optical coherence upon traversing optical systems or media that couple multiple DoFs, and suggests new applications that may exploit the coherence rank in optical imaging and communications.

Vector-space formulation of partially coherent optical fields. The most general state of an optical field characterized by a binary DoF is described by a 2×2 coherence matrix. The polarization coherence matrix is $\mathbf{G}_{\rm p}=\begin{pmatrix} G^{\rm HH} & G^{\rm HV} \\ G^{\rm VH} & G^{\rm VV} \end{pmatrix}$, where $G^{ij}=\langle E^i(E^j)^*\rangle$, $i,j={\rm H,V}$,

and E^i is a scalar field component at a point. Similarly, the spatial coherence matrix at two points a and b in a scalar field is $\mathbf{G}_\mathrm{s} = \begin{pmatrix} G_{aa} & G_{ab} \\ G_{ba} & G_{bb} \end{pmatrix}$, where $G_{kl} = \langle E_k E_l^* \rangle$, $k, l = a, b$, and E_k is the scalar field at a point. The polarization entropy is $S_\mathrm{p} = -\lambda_1 \log_2 \lambda_1 - \lambda_2 \log_2 \lambda_2$, where λ_1 and λ_2 are the eigenvalues of $\mathbf{G}_\mathrm{p}$; the spatial entropy S_s associated with $\mathbf{G}_\mathrm{s}$ is similarly defined. In general $0 \leq S_\mathrm{p}, S_\mathrm{s} \leq 1$, with $S_\mathrm{p}, S_\mathrm{s} = 0$ in the case of fully coherent fields (no statistical fluctuations) [32]. The maximum entropy is 1 bit when the field is unpolarized or spatially incoherent $\mathbf{G}_\mathrm{p}, \mathbf{G}_\mathrm{s} = \frac{1}{2}\mathcal{I}$ (where $\mathcal{I}$ is the identity matrix).

Taking *both* DoFs (i.e., two points in a vector field), the first-order coherence is described by a 4×4 coherence matrix $\mathbf{G}$ [6, 8, 16],

$$\mathbf{G} = \begin{pmatrix} G_{aa}^{\mathrm{HH}} & G_{aa}^{\mathrm{HV}} & G_{ab}^{\mathrm{HH}} & G_{ab}^{\mathrm{HV}} \\ G_{aa}^{\mathrm{VH}} & G_{aa}^{\mathrm{VV}} & G_{ab}^{\mathrm{VH}} & G_{ab}^{\mathrm{VV}} \\ G_{ba}^{\mathrm{HH}} & G_{ba}^{\mathrm{HV}} & G_{bb}^{\mathrm{HH}} & G_{bb}^{\mathrm{HV}} \\ G_{ba}^{\mathrm{VH}} & G_{ba}^{\mathrm{VV}} & G_{bb}^{\mathrm{VH}} & G_{bb}^{\mathrm{VV}} \end{pmatrix}, \tag{1}$$

where $G_{kl}^{ij} = \langle E_k^i (E_l^j)^* \rangle$, $i, j = \mathrm{H}, \mathrm{V}$, and $k, l = a, b$. The coherence matrices $\mathbf{G}$, $\mathbf{G}_\mathrm{s}$, and $\mathbf{G}_\mathrm{p}$ are all Hermitian, positive semi-definite, unity-trace matrices. A 4×4 unitary $\hat{U}$ spanning both DoFs [16] diagonalizes $\mathbf{G}$: $\mathbf{G}_\mathrm{D} = \hat{U}\mathbf{G}\hat{U}^\dagger = \mathrm{diag}\{\lambda_1, \lambda_2, \lambda_3, \lambda_4\}$, with $\sum_j \lambda_j = 1$, and the field can carry up to 2 bits of entropy $S = -\sum_{j=1}^{4} \lambda_j \log_2 \lambda_j$, where $0 \leq S \leq 2$ and $\mathrm{diag}\{\cdot\}$ refers to a diagonal matrix with the listed elements along the diagonal. If, and only if, $\lambda_1\lambda_4 = \lambda_2\lambda_3$ can $\mathbf{G}_\mathrm{D}$ be separated into a direct product with respect to the two DoFs, $\mathbf{G}_\mathrm{D} = \mathrm{diag}\{\psi_a, \psi_b\} \otimes \mathrm{diag}\{\gamma^\mathrm{H}, \gamma^\mathrm{V}\}$, where each 2×2 coherence matrix corresponds to one DoF [33]. The condition $\lambda_1\lambda_4 = \lambda_2\lambda_3$ therefore delineates optical fields that can – in principle – be rendered separable with respect to their DoFs via unitaries.

We introduce the reduced coherence matrices that result from 'tracing out' one DoF from $\mathbf{G}$: the reduced spatial coherence matrix $\mathbf{G}_\mathrm{s}^{\mathrm{red.}}$ after tracing out polarization, and the reduced polarization coherence matrix $\mathbf{G}_\mathrm{p}^{\mathrm{red.}}$ after tracing over space. We define entropies S_s and S_p for $\mathbf{G}_\mathrm{s}^{\mathrm{red.}}$ and $\mathbf{G}_\mathrm{p}^{\mathrm{red.}}$, respectively; in general, $S \leq S_\mathrm{s} + S_\mathrm{p}$, with equality occurring only when the field is separable. Crucially, whereas S is invariant with respect to global unitaries, S_s and S_p are *not*. Indeed, whereas $\mathbf{G}$ suffices to completely identify the field coherence, these reduced matrices do *not* [6, 16, 29, 34].

Coherence rank and entropy concentration. We classify these optical fields into four families according to their *coherence rank*, $\mathcal{R}(\mathbf{G})$, defined as the number of non-zero eigenvalues of $\mathbf{G}$. Rank-1 fields, $\{\lambda\} = \{1, 0, 0, 0\}$, comprise fully coherent fields, $S = 0$ (no statistical fluctuations). It is *always* possible to render rank-1 fields separable via a unitary: $\mathbf{G} \to \mathbf{G}_\mathrm{D} = \mathrm{diag}\{1, 0\} \otimes \mathrm{diag}\{1, 0\}$, whereupon both DoFs are fully coherent.

Partially coherent rank-2 fields, $\{\lambda\} = \{\lambda_1, \lambda_2, 0, 0\}$, with entropy in the range $0 < S \leq 1$, can *always* be transformed unitarily into the separable form: $\mathbf{G}_\mathrm{D} = \mathrm{diag}\{1, 0\} \otimes \mathrm{diag}\{\lambda_1, \lambda_2\}$. This corresponds to a partially polarized field that is fully coherent spatially ($S_\mathrm{p} = S$ and $S_\mathrm{s} = 0$). Alternatively, the field can be converted into a fully polarized field that is partially coherent spatially ($S_\mathrm{p} = 0$ and $S_\mathrm{s} = S$). In general, the entropy of a rank-2 field is shared between the two DoFs. Nevertheless, even in its highest-entropy state $S = 1$, $\{\lambda\} = \{\frac{1}{2}, \frac{1}{2}, 0, 0\}$, such fields can always be rendered separable such that one DoF is fully coherent (ridding it completely from statistical fluctuations), with the 1 bit of field entropy concentrated in the other DoF [29–31]; see Fig. 1.

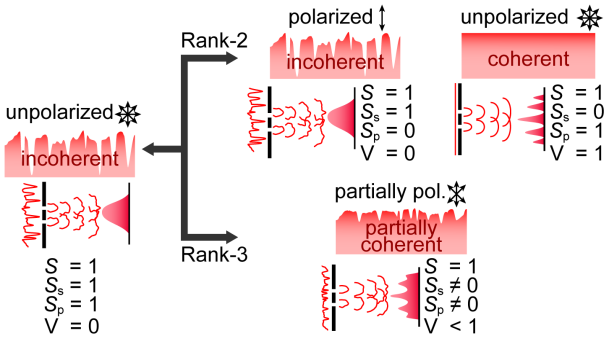

FIG. 1. Starting with a non-separable field with 1 bit of entropy ($S = 1$, left) that is unpolarized $S_\mathrm{p} = 1$ and spatially incoherent $S_\mathrm{s} = 1$, a unitary can reversibly convert it into one of two forms depending on the rank of $\mathbf{G}$. For a rank-2 field, the entropy can be *always* fully concentrated into one DoF, leaving the other DoF free of statistical fluctuations. For a rank-3 field, entropy can *never* be fully concentrated in one DoF. There always remains 'locked entropy' in the other DoF.

In stark contrast, the coherence matrices associated with rank-3 fields, $\{\lambda\} = \{\lambda_1, \lambda_2, \lambda_3, 0\}$, whose entropy is in the range $0 < S \leq 1.585$, can*not* be expressed as a direct product ($\lambda_1\lambda_4 = 0 \neq \lambda_2\lambda_3$); that is, rank-3 fields are *never* separable with respect to their DoFs. This fundamental non-separability is independent of the values $\{\lambda\}$ and is solely a consequence of the rank of $\mathbf{G}$. This hitherto unrecognized feature has important consequences for entropy concentration: it prevents ridding either DoF altogether from statistical fluctuations. Indeed, after concentrating the entropy into one DoF, a residual amount of entropy is retained that we refer to as *locked entropy*. The entropy in a rank-3 field must always be shared between the DoFs no matter how low S is. Even when $S < 1$, it is impossible to realize the condition $S_\mathrm{p} = S$ and $S_\mathrm{s} = 0$ (or $S_\mathrm{p} = 0$ and $S_\mathrm{s} = S$) unitarily, which is attainable for rank-2 fields *of the same entropy* [Fig. 1]. Furthermore, when $S > 1$ one cannot concentrate 1 bit of entropy in one of the DoFs. Defining the function $f(x) = -x \log_2 x - (1-x) \log_2 (1-x)$, the minimum entropy that is locked in one DoF is $S_\mathrm{min} = f(\lambda_1 + \lambda_2)$, in which case the entropy concentrated into the other DoF is $S_\mathrm{max} = f(\lambda_1 + \lambda_3)$.

Rank-4 fields, $\{\lambda\} = \{\lambda_1, \lambda_2, \lambda_3, \lambda_4\}$, can sometimes be unitarily rendered separable with respect to their DoFs

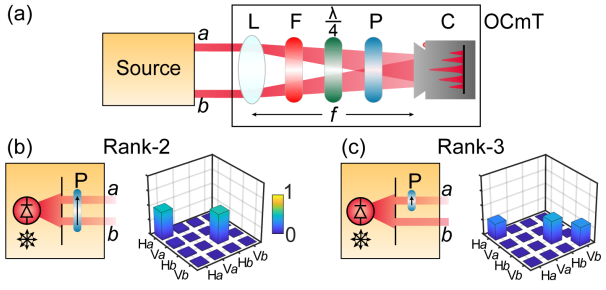

FIG. 2. (a) Schematic of the OCmT measurement scheme used to measure coherence matrices; L: spherical lens (focal length $f = 30$ cm); F: spectral filter; $\frac{\lambda}{4}$: quarter wave plate; P: linear polarizer; C: CMOS camera. (b) Source preparation for a rank-2 field and the measured 4×4 coherence matrix $\mathbf{G}$. (c) Same as (b) for a rank-3 field.

depending on the eigenvalues, and they thus share the properties of rank-2 or rank-3 fields. Recalling the condition mentioned above that potentially separable fields satisfy $\lambda_1\lambda_4 = \lambda_2\lambda_3$, we can show that some rank-4 fields can be made separable while others cannot. For example, a field with $\{\lambda\} = 0.25 * \{1, 1, 1, 1\}$ can be rendered separable using unitaries, but a field with $\{\lambda\} = \{0.7, 0.1, 0.1, 0.1\}$ cannot. Given the focus of the work presented here, we do not examine rank-4 fields, and focus instead on delineating the characteristics of rank-2 and rank-3 fields.

Experiment. We first prepare and characterize representative rank-2 and rank-3 fields [Fig. 2]. Starting from unpolarized, spatially incoherent light from an LED (wavelength 625 nm), we select two spatial modes using slits at points a and b that are sufficiently separated to guarantee mutual incoherence [Fig. 2(a)]. For a rank-2 field $\mathbf{G} = \frac{1}{2}\mathrm{diag}\{1, 0, 1, 0\}$, the source configuration along with the measured coherence matrix are shown in Fig. 2(b), and the corresponding results for the rank-3 field with $\mathbf{G} = \frac{1}{3}\mathrm{diag}\{1, 0, 1, 1\}$ are shown in Fig. 2(c). The rank-2 field is prepared by placing a polarizer at both a and b, yielding $S = 1$: the field is polarized $S_\mathrm{p} = 0$ but spatially incoherent $S_\mathrm{s} = 1$. The rank-3 field is prepared by placing a linear polarizer at b only (the field at a remains unpolarized) to yield $S = 1.585$: the field is partially polarized and partially coherent spatially. Throughout, $\mathbf{G}$ is reconstructed via optical coherence matrix tomography (OCmT) [Fig. 2(a)], which extends to optical fields with multiple DoFs [34, 35] the analogous procedure of quantum state tomography [36–38]; see Supplementary for further experimental details [39].

The impact of the coherence rank on the limits of entropy concentration is illustrated in Fig. 3. We consider iso-entropy (i.e., equal in entropy) rank-2 [Fig. 3(a)] and rank-3 [Fig. 3(b)] fields. We make use of an entropy converter that unitarily couples the two DoFs [Fig. 3(c)], which comprises a half-wave plate (HWP) W_1 in path a oriented at 45° with respect to H (H→V, V→H), a polarizing beam splitter (PBS) that couples modes a and b

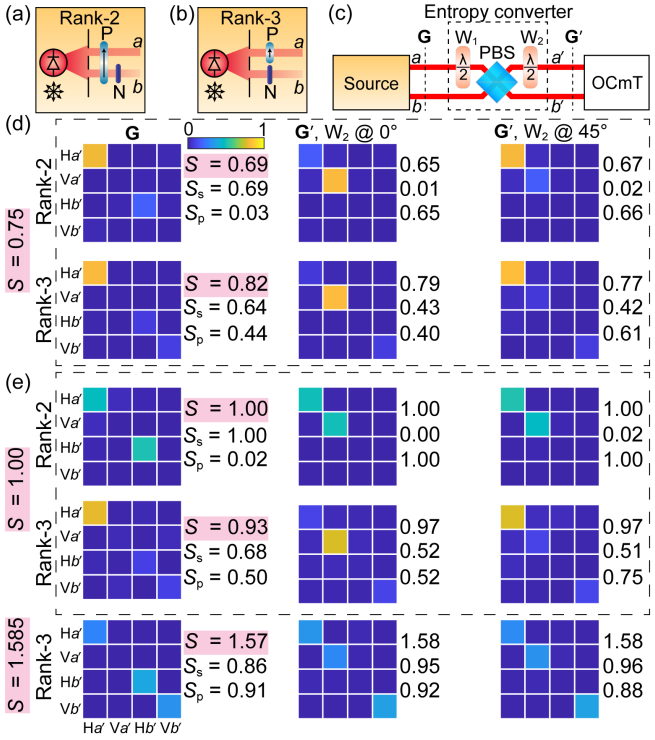

FIG. 3. Unitary entropy conversion for rank-2 and rank-3 fields. (a) Source configurations for rank-2 and (b) rank-3 fields. P: Linear polarizer oriented along H; N: neutral density filter. (c) Setup for entropy conversion. W: Half-wave plate; PBS: polarizing beam splitter. (d-f) From left to right: $\mathbf{G}$ reconstructed before the entropy converter; $\mathbf{G}'$ after the entropy converter with W_2 oriented at 0°; and $\mathbf{G}'$ with W_2 at 45°. All matrices are measurements, and the fidelity throughout was >98% with respect to theoretical expectations (see Supplementary [39]). (d) Rank-2 and rank-3 fields with $S \approx 0.75$; (e) same as (d) for $S \approx 1$; and (f) rank-3 field with $S \approx 1.585$.

and produces modes a' and b', followed by a HWP W_2 in mode a' in one of two orientations: at 0° with H (H→H and V→ −V), and at 45° with H (H→V, V→H). The first orientation minimizes the entropy in the spatial DoF (entropy concentration), while the second orientation swaps the entropy of the spatial and polarization DoFs (entropy swapping).

Either binary DoF (polarization or spatial modes) can support up to 1 bit of entropy. We thus first prepare rank-2 and rank-3 fields with $S = 0.75$ [Fig. 3(d)]. For the rank-2 field, the entire entropy can be concentrated in the spatial DoF, $S_\mathrm{s} = 0.75$ (partially coherent spatially) and $S_\mathrm{p} = 0$ (fully polarized). Using the first setting for W_2, the entropy converter minimizes the spatial entropy: $S_\mathrm{s} \to 0$ (spatially coherent) and $S_\mathrm{p} \to 0.75$ (partially polarized). The second setting for W_2 swaps the entropy between the DoFs, which yields here the same result as that of entropy concentration with the first setting.

The corresponding results for the rank-3 field are entirely in contrast to those for the iso-entropy $S = 0.75$ rank-2 field. The rank-3 source configuration yields the-

oretical values of $S_s = 0.6$ (partially coherent spatially) and $S_p = 0.38$ (partially polarized); see Supplementary [39]. The first setting minimizes the spatial entropy but can*not* concentrate all the entropy into the polarization DoF; rather, some entropy remains locked in the spatial DoF $S_s \to 0.38$. The second setting for the entropy converter swaps the entropy between the DoFs: $S_s \to 0.38$ (partially coherent spatially) and $S_p \to 0.6$ (partially polarized). Similar results are obtained when the initial field has a total of 1 bit of entropy, $S = 1$ [Fig. 3(e)]. Whereas the entire entropy can be concentrated in either DoF in the case of a rank-2 field, this cannot be achieved for the iso-entropy rank-3 field, and some entropy must remain locked in either DoF. Finally, the entropy of rank-3 can exceed 1 bit (whereas that of rank-2 fields cannot). In Fig. 3(f) we repeat the measurements with a maximum-entropy rank-3 field, $S = 1.585$. Here the locked entropy in the spatial DoF is $S_s = f(\frac{2}{3}) = 0.92$.

The field rank can be identified by reconstructing $\mathbf{G}$, as shown in Fig. 3. Nevertheless, information concerning the coherence rank can be deduced by observing the visibility of the spatial interference fringes produced by the field when the fields at a and b are superposed after a polarization projection. Two theorems (see Supplementary for proofs [39]) help establish a strategy for this approach.

Theorem 1. *For a vector optical field supported on two spatial points with a coherence matrix* $\mathbf{G}$*, if there exists a polarization projection along vector* $\mathbf{P}$ *along which the field is spatially coherent (i.e., it can produce spatial interference fringes with* 100% *visibility), then* $\mathcal{R}(\mathbf{G}) \leq 3$.

Theorem 2. *For a vector optical field supported on two points with a coherence matrix* $\mathbf{G}$*, if there exist two orthogonal polarization projections* $\mathbf{P}$ *and* $\mathbf{Q}$ *along which the field is spatially coherent (i.e., it can produce* 100%*-visibility spatial interference fringes), then* $\mathcal{R}(\mathbf{G}) \leq 2$.

In other words, identifying an orthogonal pair of polarization projections that both yield a spatially coherent field indicates that the field is either rank-1 or rank-2. Identifying only a single polarization projection that yields a spatially coherent field indicates that the field is rank-3. There is *no* polarization projection for a rank-4 field that yields a spatially coherent field.

We demonstrate these results experimentally in Fig. 4 with pairs of iso-entropy rank-2 and rank-3 fields. After the field is prepared, it is directed through the entropy converter shown in Fig. 3(c), and then the field is globally projected onto a prescribed polarization. We search for pairs of directions along which the resulting scalar field yields spatial interference fringes with 100% visibility.

We start with a pair of fields at $S \approx 0.75$ [Fig. 4(a)]. The rank-2 field is prepared by projecting the polarization at 45° with respect to H and adjusting the amplitude of one spatial mode to obtain the targeted entropy (see Supplementary [39] for the full coherence matrices associated with the fields in Fig. 4). After the entropy converter with W_2 oriented at 0°, no spatial interference fringes of high visibility are observed at any polarization projection. After setting W_2 at 45°, the polarization projections along H and V yield high-visibility spatial interference fringes, as expected for a rank-2 field.

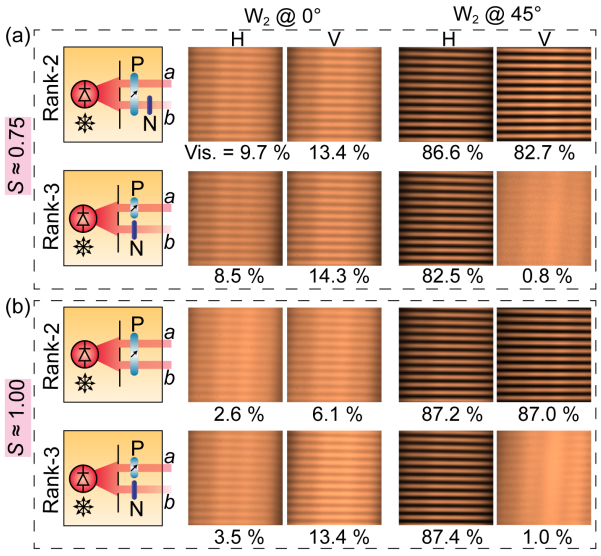

FIG. 4. Identifying the coherence rank through the spatial coherence after a polarization projection. (a,b) From left to right: the source preparation; optimal interference fringes along the H and V polarization projections after the entropy converter in Fig. 3(c), with W_2 oriented at 0° with H; and optimal interference fringes along the H and V polarization projections with W_2 oriented at 45°. (a) Iso-entropy rank-2 and rank-3 fields with $S = 0.75$. (b) Same as (a) for $S = 1$.

We contrast these observations with those for an iso-entropy rank-3 field $S \approx 0.75$. This field is prepared by projecting the polarization at a alone along 45° and adjusting the amplitude at b to obtain the target entropy. After the entropy converter with W_2 oriented at 0°, no spatial interference fringes are observed at any polarization projection. However, after setting W_2 at 45°, projecting the polarization along H yields a field that produces high-visibility spatial interference fringes. The corresponding polarization projection along V does *not* yield a spatially coherent field, and no interference fringes can be observed. We increase the field entropy for an iso-entropy pair of rank-2 and rank-3 fields to $S \approx 1$ (the maximum entropy for rank-2) [Fig. 4(b)], and observe similar results to those for the lower-entropy fields [Fig. 4(a)]. Despite the higher entropy, we can still identify a pair of polarization projections for the rank-2 field that result in spatial coherence, whereas only a single polarization projection is identified for the rank-3 field.

Discussion. The approach outlined here in terms of coherence matrices [8, 40–42] reveals features that are difficult to discern otherwise when extended to multiple DoFs. The analysis and experiments suggest a wealth of fundamental questions regarding the statistical behavior of optical fields: How does the rank vary spatially across a vector optical field? How does the spatial distribution

of the rank evolve with free propagation? How is the coherence rank affected by optical nonlinearities? Although we have couched the coherence matrix here in terms of polarization and spatial modes, this description can be extended to other DoFs, including higher-dimensional DoFs (e.g., orbital angular momentum), and even continuous DoFs after implementing the Schmidt decomposition to obtain an effective finite-dimensional representation [25, 43–46]. This is particularly relevant in light of recent realizations of optical fields in which the spatial, temporal, and polarization DoFs are all coupled [47–50]. In addition to the intrinsic interest of the coherence rank as a potential thermodynamic variable for electromagnetic fields, it may also serve as an integer identifier of the global properties of the field to be exploited for communications schemes using partially coherent light [51]. As previously mentioned, the coherence matrix may be extended to continuous DoFs, thus scaling up the rank to correspond to a large-dimensional alphabet of symbols to be used for engineering encoding schemes in optical communications. In prior work, we explored the application of rank-2 fields in protecting DoFs from decohering effects [29, 30].

In conclusion, we have presented a classification scheme of partially coherent optical fields based on the rank of the 4×4 coherence matrix for two binary DoFs. This classification unveils surprising structural distinctions: *all* rank-2 fields are fundamentally separable whereas all rank-3 fields are intrinsically *non*-separable. Consequently, the entropy in rank-2 fields – no matter how high – can always be concentrated into one DoF, thereby leaving the other DoF free of statistical fluctuations. In contrast, in a rank-3 field the entropy – no matter how low – cannot be fully concentrated into one DoF, and locked entropy remains associated with the other DoF.

ACKNOWLEDGMENTS

We thank C. Okoro, M. Yessenov, and A. Dogariu for useful discussions and assistance. This work was funded by the US Office of Naval Research (ONR) under contracts N00014-17-1-2458 and N00014-20-1-2789.

[1] F. Zernike, Physica **5**, 785 (1938).
[2] L. Mandel and E. Wolf, Rev. Mod. Phys. **37**, 231 (1965).
[3] L. Mandel and E. Wolf, *Optical Coherence and Quantum Optics* (Cambridge Univ. Press, Cambridge, 1995).
[4] E. Wolf, *Introduction to the Theory of Coherence and Polarization of Light* (Cambridge Univ. Press, Cambridge, 2007).
[5] X.-F. Qian and J. H. Eberly, Opt. Lett. **36**, 4110 (2011).
[6] K. H. Kagalwala, G. Di Giuseppe, A. F. Abouraddy, and B. E. A. Saleh, Nat. Photon. **7**, 72 (2013).
[7] F. Gori, Opt. Lett. **23**, 241 (1998).
[8] F. Gori, M. Santarsiero, and R. Borghi, Opt. Lett. **31**, 858 (2006).
[9] F. Gori, M. Santarsiero, and R. Borghi, Opt. Lett. **32**, 588 (2007).
[10] R. J. C. Spreeuw, Found. Phys. **28**, 361 (1998).
[11] R. J. C. Spreeuw, Phys. Rev. A **63**, 062302 (2001).
[12] A. Aiello, F. Töppel, C. Marquardt, E. Giacobino, and G. Leuchs, New J. Phys. **17**, 043024 (2015).
[13] A. Forbes, A. Aiello, and B. Ndagano, Prog. Opt. **64**, 99 (2019).
[14] T. Konrad and A. Forbes, Contemp. Phys. **60**, 1 (2019).
[15] B. N. Simon, S. Simon, F. Gori, M. Santarsiero, R. Borghi, N. Mukunda, and R. Simon, Phys. Rev. Lett. **104**, 023901 (2010).
[16] A. F. Abouraddy, Opt. Express **25**, 18320 (2017).
[17] B. Ndagano, B. Perez-Garcia, F. S. Roux, M. McLaren, C. Rosales-Guzman, Y. Zhang, O. Mouane, R. I. Hernandez-Aranda, T. Konrad, and A. Forbes, Nat. Phys. **13**, 397 (2017).
[18] E. Otte, C. Rosales-Guzmán, B. Ndagano, C. Denz, and A. Forbes, Light Sci. Appl. **7**, 18009 (2018).
[19] S. Mamani, L. Shi, T. Ahmed, R. Karnik, A. Rodríguez-Contreras, D. Nolan, and R. Alfano, J. Biophoton. **11**, e201800096 (2018).
[20] H. E. Kondakci, M. A. Alonso, and A. F. Abouraddy, Opt. Lett. **44**, 2645 (2019).
[21] E. Toninelli, B. Ndagano, A. Vallés, B. Sephton, I. Nape, A. Ambrosio, F. Capasso, M. J. Padgett, and A. Forbes, Adv. Opt. Photon. **11**, 67 (2019).
[22] Yao-Li, X.-B. Hu, B. Perez-Garcia, Bo-Zhao, W. Gao, Z.-H. Zhu, and C. Rosales-Guzmán, Appl. Phys. Lett. **116**, 221105 (2020).
[23] Y. Shen, I. Nape, X. Yang, X. Fu, M. Gong, D. Naidoo, and A. Forbes, Light Sci. Appl. **10**, 50 (2021).
[24] Y. Shen, A. Zdagkas, N. Papasimakis, and N. I. Zheludev, Phys. Rev. Res. **3**, 013236 (2021).
[25] L. A. Hall and A. F. Abouraddy, J. Opt. Soc. Am. A **39**, 2016 (2022).
[26] A. Aiello, X.-B. Hu, V. Rodríguez-Fajardo, A. Forbes, R. I. Hernandez-Aranda, B. Perez-Garcia, and C. Rosales-Guzmán, New J. Phys. **24**, 063032 (2022).
[27] A. Halder, A. Norrman, and A. T. Friberg, Opt. Lett. **46**, 5619 (2021).
[28] K. H. Kagalwala, G. Di Giuseppe, A. F. Abouraddy, and B. E. A. Saleh, Nat. Commun. **8**, 739 (2017).
[29] C. Okoro, H. E. Kondakci, A. F. Abouraddy, and K. C. Toussaint, Optica **4**, 1052 (2017).
[30] M. Harling, V. Kelkar, C. Okoro, M. Diouf, A. F. Abouraddy, and K. C. Toussaint, Opt. Express **30**, 29584 (2022).
[31] M. Harling, V. Kelkar, A. F. Abouraddy, and K. C. Toussaint, J. Opt. **25**, 053502 (2023).
[32] C. Brosseau and A. Dogariu, Prog. Opt. **49**, 315 (2006).
[33] A. F. Abouraddy, B. E. A. Saleh, A. V. Sergienko, and M. C. Teich, Phys. Rev. A **64**, 050101(R) (2001).
[34] K. H. Kagalwala, H. E. Kondakci, A. F. Abouraddy, and B. E. A. Saleh, Sci. Rep. **5**, 15333 (2015).

[35] A. F. Abouraddy, K. H. Kagalwala, and B. E. A. Saleh, Opt. Lett. **39**, 2411 (2014).
[36] W. K. Wootters, in *Complexity, Entropy, and the Physics of Information*, SFI Studies in the Sciences of Complexity, Vol. VIII, edited by W. H. Zurek (Addison-Wesley, Reading, 1990) pp. 39–46.
[37] D. F. V. James, P. G. Kwiat, W. J. Munro, and A. G. White, Phys. Rev. A **64**, 052312 (2001).
[38] A. F. Abouraddy, A. V. Sergienko, B. E. A. Saleh, and M. C. Teich, Opt. Comm. **201**, 93 (2002).
[39] See Supplemental Material at [URL will be inserted by publisher] for a detailed description of the experimental setup in Fig. 2, details on OCmT, and theoretical results.
[40] U. Fano, Rev. Mod. Phys. **29**, 74 (1957).
[41] H. Gamo, Prog. Opt. **3**, 187 (1964).
[42] J. Perina, *Coherence of light* (Springer, 1985).
[43] A. Ekert and P. L. Knight, Am. J. Phys. **63**, 415 (1995).
[44] C. K. Law, I. A. Walmsley, and J. H. Eberly, Phys. Rev. Lett. **84**, 5304 (2000).
[45] C. K. Law and J. H. Eberly, Phys. Rev. Lett. **92**, 127903 (2004).
[46] J. H. Eberly, Laser Phys. **16**, 921 (2006).
[47] M. Diouf, M. Harling, M. Yessenov, L. A. Hall, A. F. Abouraddy, and K. C. Toussaint, Opt. Express **29**, 37225 (2021).
[48] M. Yessenov, J. Free, Z. Chen, E. G. Johnson, M. P. Lavery, M. A. Alonso, and A. F. Abouraddy, Nature Communications **13**, 1 (2022).
[49] M. Yessenov, L. A. Hall, K. L. Schepler, and A. F. Abouraddy, Adv. Opt. Photon. **14**, 455 (2022).
[50] M. Yessenov, Z. Chen, M. P. J. Lavery, and A. F. Abouraddy, Opt. Lett. **47**, 4131 (2022).
[51] A. Nardi, S. Divitt, M. Rossi, F. Tebbenjohanns, A. Militaru, M. Frimmer, and L. Novotny, Opt. Lett. **47**, 4588 (2022).